



# A Novel Sparse Representation Method for Image Restoration Applications

K.S.K.L.Priyanka, U.V.Ratna Kumari

Department of ECE,  
Jawaharlal Nehru Technological University Kakinada (JNTUK),  
Kakinada, India  
priyanka.kskl@gmail.com, vinayratna74@gmail.com

**Abstract**—Sparse representation has been widely used in various image restoration applications. The quality of image restoration mainly depends on whether the used sparse domain can represent well the underlying image. Since the contents representing the underlying image can vary significantly across different images or different patches in an image, we propose to learn various sets of bases from a pre-collected dataset of example image patches and for processing a particular given patch, a suitable set of base is selected adaptively as local sparse domain. Here we introduce two adaptive regularization terms into the sparse representation framework. One is a set of auto regressive (AR) models are learned from the pre-collected dataset of example image patches and the best fitted AR model is adaptively selected for regularization. Second is image non-local self similarity regularization to regularize the image local structures. To make the sparse coding more accurate, a centralized sparsity constraint is introduced by exploiting the nonlocal image statistics. The local sparsity and the nonlocal sparsity constraints are unified into a variational framework for optimization. Extensive experiments on the proposed method of CSR method achieves convincing improvement over previous state-of-the-art methods in terms of PSNR and SSIM values.

**Keywords**-----Image restoration, deblurring, super-resolution, sparse representation, regularization

## INTRODUCTION

Image restoration (IR) aims to recover a high-quality image from its degraded (e.g., noisy, blurred and/or downsampled) versions, which may be taken, for example, by a low-end camera and/or under limited conditions. For an observed image  $Y$ , the problem of IR can be expressed by

$$Y = DHX + v \quad ..(1)$$

where  $X$  is the unknown image to be estimated, and  $H$  and  $D$  are degrading operators and  $v$  is additive noise. When  $H$  and  $D$  are identities, the IR problem becomes denoising; when  $D$  is identity and  $H$  is a blurring operator, IR becomes deblurring; when  $D$  is identity and  $H$  is a set of random projections, IR becomes compressed sensing[3]; when  $D$  is a down-sampling operator and  $H$  is a blurring operator, IR becomes (single-image) super-resolution. IR, a fundamental problem in image processing has been widely studied in the past three decades. In this paper, we focus on deblurring and single-image super-resolution.

Due to the ill-posed nature of IR[2], the solution to (1) with an  $l_2$ -norm fidelity constraint, i.e.,

$$\hat{X} = \arg \min_x \|Y - DHX\|_2^2 \text{ is generally not unique. A}$$

prior knowledge of natural images can be used to regularize the IR problem for finding a better solution. One of the most commonly used regularization models is the total variation (TV) model

$$\hat{X} = \arg \min_x \left\{ \|Y - DHX\|_2^2 + \lambda \|\nabla X\|_1 \right\} ,$$

where  $\|\nabla X\|_1$  is the  $l_1$ -norm of the first-order derivative of  $X$  and  $\lambda$  is a constant.

The success of TV regularization validates the importance of good image prior models in solving the IR problems. In wavelet based image denoising the sparsity of wavelet coefficients can serve as good prior. This reveals the fact that many types of signals, e.g., natural images, can be sparsely represented (or coded) using a dictionary of atoms, such as DCT or wavelet bases, that is, denoting by  $\Phi$  the dictionary, we have  $X \approx \Phi\alpha$  and most of the coefficients in  $\alpha$  are close to zero. With the sparsity prior, the representation of  $X$  over  $\Phi$  can be estimated from its observation  $Y$  by solving the following  $l_0$ -minimization problem:

$$\hat{\alpha} = \arg \min_{\alpha} \left\{ \|Y - DH\Phi\alpha\|_2^2 + \lambda \|\alpha\|_0 \right\} ,$$

where the  $l_0$ -norm counts the number of nonzero coefficients in vector  $\alpha$ . Once we obtain  $\hat{\alpha}$ ,  $X$  can then be estimated as  $\hat{X} = \Phi\hat{\alpha}$ . The  $l_0$ -minimization is an NP-hard combinatorial search problem, and is usually solved by greedy algorithms. The  $l_1$ -minimization, as the closest convex function to  $l_0$ -minimization, is then widely used as an alternative approach to solving the sparse coding

problem:  $\hat{\alpha} = \arg \min_{\alpha} \left\{ \|Y - DH\Phi\alpha\|_2^2 + \lambda \|\alpha\|_1 \right\}$ . For

better IR results the  $l_1$ -norm sparsity regularization term has been iteratively reweighted. Sparse representation has been successfully used in various image processing applications.

The main issue in sparse representation modeling is the determination of dictionary  $\Phi$ . Many dictionary learning (DL) methods aim at learning a universal and over-complete dictionary to represent various image structures. However, sparse decomposition over a highly redundant

dictionary is potentially unstable and tends to generate visual artifacts. In this paper, we propose an adaptive sparse domain selection (ASDS) scheme for sparse representation. A set of compact subdictionaries is learned from high-quality example image patches. The example image patches are clustered into many clusters. Since each cluster consists of many patches with similar patterns, a compact subdictionary can be learned for each cluster. Particularly, for simplicity, we use the principal component analysis (PCA) technique to learn the subdictionaries. For an image patch to be coded, the best subdictionary that is most relevant to the given patch is selected. Since the given patch can be better represented by the adaptively selected subdictionary, the whole image can be more accurately reconstructed than using a universal dictionary, which will be validated by our experiments.

In addition to sparsity regularization, we introduce other regularization terms to further increase the IR performance. Here, we propose to use the piecewise autoregressive (AR) models, that are prelearned from the training dataset, to characterize the local image structures. For each given local patch, one or more AR models can be adaptively selected for regularization. On the other hand, considering the fact that there are often many repetitive image structures in an image, we introduce a nonlocal (NL) self-similarity constraint served as another regularization term, which preserves edge sharpness and suppresses noise.

We use an efficient iterative shrinkage (IS) algorithm to solve the  $l_1$ -minimization problem after adding ASDS and adaptive regularizations (AReg) into the sparse representation based IR framework. In addition, we adaptively estimate the image local sparsity to adjust the sparsity regularization parameters. In addition, we propose a centralized sparse representation (CSR) model to effectively reduce the sparse coding noise (SCN) (difference of original image and estimated image) and thus enhance the sparsity based IR performance. The basic idea is to integrate the image local sparsity constraint (i.e., a local patch can be coded by a few atoms sparsely selected from a dictionary) and the centralized sparsity constraint (i.e., the sparse coding coefficients should be close to their mean values) into a unified variational framework for optimization. Extensive experiments on IR are conducted, and the experimental results show that the proposed CSR algorithm outperforms significantly many state-of-the-art IR methods in terms of PSNR and SSIM values.

**PRIOR ART**

In recent years, sparse coding or sparse representation strategy has been widely studied to solve inverse problems, partially due to the progress of  $l_0$ -norm and  $l_1$ -norm minimization techniques .

Let  $X \in \mathfrak{R}^n$  is the target signal to be coded, and  $\Phi = [\phi_1, \dots, \phi_m] \in \mathfrak{R}^{n \times m}$  is a given dictionary of atoms (i.e., code set). The sparse coding of X over  $\Phi$  is to find a sparse vector  $\alpha = [\hat{a}_1, \dots, \hat{a}_m]$  (i.e., most of the coefficients in  $\alpha$  are close to zero) such that  $X \approx \Phi\alpha$  . If the sparsity is measured as the  $l_0$ -norm of  $\alpha$  , which counts the nonzero coefficients in  $\alpha$  , the sparse coding problem becomes

$$\min_{\alpha} \|X - \Phi\alpha\|_2^2 \text{ s.t. } \|\alpha\|_0 \leq T \text{ , where } T \text{ is a scalar}$$

controlling the sparsity. Alternatively, the sparse vector can also be found by

$$\hat{\alpha} = \arg \min_{\alpha} \{ \|X - \Phi\alpha\|_2^2 + \lambda \|\alpha\|_0 \} \quad (2)$$

where  $\lambda$  is a constant. Since the  $l_0$ -norm is nonconvex, it is often replaced by either the standard  $l_1$ -norm or the weighted  $l_1$ -norm to make the optimization problem convex.

The critical issue sparse representation modelling is the selection of dictionary  $\Phi$  . Given a set of training image patches  $S = [s_1, \dots, s_N] \in \mathfrak{R}^{n \times N}$  , dictionary learning (DL) aims to jointly optimize the dictionary  $\Phi$  and the representation coefficient matrix  $\Lambda = [\alpha_1, \dots, \alpha_N]$  such that  $s_i \approx \Phi\alpha_i$  and  $\|\alpha_i\|_p \leq T$  , where  $p = 0$  or  $1$ . This can be formulated by the following minimization problem:

$$(\hat{\Phi}, \hat{\Lambda}) = \arg \min_{\Phi, \Lambda} \|S - \Phi\Lambda\|_F^2 \text{ s.t. } \|\alpha_i\|_p \leq T, \forall_i \quad (3)$$

where  $\|\cdot\|_F$  is the Frobenius norm. The above minimization problem is nonconvex even when  $p = 1$  . To make it tractable, approximation approaches, including MOD and K-SVD ,have been proposed to alternatively optimizing  $\Phi$  and  $\Lambda$  , leading to many state-of-the-art results in image processing.

Regularization has been used in IR for a long time to incorporate the image prior information. As a classic method, the autoregressive (AR) modeling has been successfully used in image compression [33] and interpolation. Recently, the AR model was used for adaptive regularization in compressive image

$$\text{recovery : } \min_X \sum_i \|X_i - \chi_i \alpha_i\|_2^2 \text{ s.t. } Y = AX \text{ , where}$$

$\chi_i$  is the vector containing the neighboring pixels of pixel  $X_i$  within the support of the AR model, and  $\alpha_i$  is the AR parameter vector. In this paper, we propose a learning-based adaptive regularization, where the AR models are learned from high-quality training images, to increase the AR modeling accuracy.

In recent years, the nonlocal (NL) methods have led to promising results in various IR tasks, especially in image denoising. The idea of NL methods is very simple: the patches that have similar patterns can be spatially far from each other, and thus we can collect them in the whole image. This NL self-similarity prior was later employed in image deblurring and super-resolution as second regularization term .

**SPARSE REPRESENTATION WITH ADAPTIVE SPARSE DOMAIN SELECTION (ASDS)**

In this section, we propose an ASDS scheme, in which a series of compact subdictionaries are learned and assigns adaptively each local patch a subdictionary as the sparse domain. With ASDS, a weighted  $l_1$ -norm sparse representation model will be proposed for IR tasks. Suppose that  $\{\Phi_k\}$ ,  $k=1,2,\dots,K$ , is a set of orthonormal subdictionaries. Let  $X$  be an image vector, and  $X_i = R_i X, i=1,2,\dots,N$ , be the  $i^{\text{th}}$  patch (size:  $\sqrt{n} \times \sqrt{n}$ ) vector of  $X$ , where  $R_i$  is a matrix extracting patch  $X_i$  from  $X$ . For patch  $X_i$ , suppose that a subdictionary  $\Phi_{k_i}$  is selected for it. Then,  $X_i$  can be approximated as  $\hat{X}_i = \Phi_{k_i} \alpha_i, \|\alpha_i\|_1 \leq T$ , via sparse coding. The whole image  $X$  can be reconstructed by averaging all of the reconstructed patches  $\hat{X}_i$ , which can be mathematically written as

$$\hat{X} = \left( \sum_{i=1}^N R_i^T R_i \right)^{-1} \sum_{i=1}^N (R_i^T \Phi_{k_i} \alpha_i). \quad (4)$$

In (4), the matrix to be inverted is a diagonal matrix, and hence the calculation of (4) can be done in a pixel-by-pixel manner. Obviously, the image patches can be overlapped to better suppress noise and block artifacts. For the convenience of expression, we define the following operator “ $\circ$ ”:

$$\hat{X} = \Phi \circ \alpha = \left( \sum_{i=1}^N R_i^T R_i \right)^{-1} \sum_{i=1}^N (R_i^T \Phi_{k_i} \alpha_i) \quad (5)$$

where  $\Phi$  is the concatenation of all subdictionaries  $\{\Phi_k\}$  and  $\alpha$  is the concatenation of all  $\alpha_i$ .

Let  $Y = DHX + v$  be the observed degraded image, our goal is to recover the original image  $X$  from  $Y$ . With ASDS and the definition in (5), the IR problem can be formulated as follows:

$$\hat{\alpha} = \arg \min_{\alpha} \left\{ \|Y - DH\Phi \circ \alpha\|_2^2 + \lambda \|\alpha\|_1 \right\} \quad (6)$$

Clearly, one key procedure in the proposed ASDS scheme is the determination of  $\Phi_{k_i}$  for each local patch. To facilitate the sparsity-based IR, we propose to learn offline the subdictionaries  $\{\Phi_k\}$ , and select online from  $\{\Phi_k\}$  the best fitted subdictionary to each patch  $X_i$ .

**A. Learning the Subdictionaries**

In order to learn a series of subdictionaries to code the various local image structures, we need to first construct a dataset of local image patches for training. For this purpose, we collected a set of high-quality natural images and cropped from them a rich amount of image patches with size  $\sqrt{n} \times \sqrt{n}$ . A cropped image patch, denoted by  $s_i$ , will be involved in DL if its intensity variance  $Var(s_i)$  is greater than a threshold  $\Delta$ , i.e.,  $Var(s_i) > \Delta$ . This patch selection criterion is to exclude the smooth patches from

training and guarantee that only the meaningful patches with a certain amount of edge structures are involved in DL. Let  $M$  image patches  $S = [s_1, s_2, \dots, s_M]$  are selected.

Now our goal is to learn  $K$  compact subdictionaries  $\{\Phi_k\}$  from  $S$  so that, for each given local image patch, the most suitable subdictionary can be selected. For this, we cluster the dataset  $S$  into  $K$  clusters, and learn a subdictionary from each of the  $K$  clusters. Apparently, the  $K$  clusters are expected to represent the  $K$  distinctive patterns in  $S$ . To generate perceptually meaningful clusters, we perform the clustering in a feature space. In the hundreds of thousands patches cropped from the training images, many patches are approximately the rotated version of the others. Since the human visual system is sensitive to image edges, which convey most of the semantic information of an image, we use the high-pass filtering output of each patch as the feature for clustering. It allows us to focus on the edges and structures of image patches without taking into account the pixel intensities and helps to increase the accuracy of clustering

Consider  $S_h = [s_1^h, s_2^h, \dots, s_M^h]$  as the high-pass filtered dataset of  $S$ . We used the K-means algorithm to partition  $S_h$  into  $K$  clusters  $\{C_1, C_2, \dots, C_K\}$  and denote by  $\mu_k$  the centroid of cluster  $C_k$ . Once  $S_h$  is partitioned, dataset  $S$  can then be clustered into  $K$  subsets  $S_k, k=1,2,\dots,K$ , and  $S_k$  is a matrix of dimension  $n \times m_k$ , where  $m_k$  denotes the number of samples in  $S_k$ .

Now we focus on how to learn a subdictionary  $\Phi_k$  from the cluster  $S_k$  such that all the elements in  $S_k$  can be faithfully represented by  $\Phi_k$ . The design of  $\Phi_k$  can be intuitively formulated by the following objective function:

$$(\hat{\Phi}_k, \hat{\Lambda}_k) = \arg \min_{\Phi_k, \Lambda_k} \left\{ \|S_k - \Phi_k \Lambda_k\|_F^2 + \lambda \|\Lambda_k\|_1 \right\} \quad (7)$$

where  $\Lambda_k$  is the representation coefficient matrix of  $S_k$  over  $\Phi_k$ . Equation (7) is a joint optimization problem of  $\Phi_k$  and  $\Lambda_k$ , and it can be solved by alternatively optimizing  $\Phi_k$  and  $\Lambda_k$  like in the K-SVD algorithm.

However, we do not directly use (7) to learn the subdictionary  $\Phi_k$  based on the following considerations.

First, the  $l_2 - l_1$  joint minimization in (7) requires much computational cost. Second, we often assume that the dictionary  $\Phi_k$  is over-complete. Nonetheless, here  $S_k$  is a subdataset after K-means clustering, which implies that, not only is the number of elements in  $S_k$  limited, but also these elements tend to have similar patterns. Therefore, it is not necessary to learn an over-complete dictionary  $\Phi_k$  from  $S_k$ . In addition, a compact dictionary will decrease much the computational cost of the sparse coding of a given image patch. For the above said reasons, we propose to

learn a compact dictionary while trying to approximate (7). So we choose PCA as good solution for this problem. PCA is a classical signal de-correlation and dimensionality reduction technique that is widely used in pattern recognition and statistical signal processing. In this paper, we apply PCA to each subdataset  $S_k$  to compute the principal components, from which the dictionary  $\Phi_k$  is constructed. Denote by  $\Omega_k$  the co-variance matrix of dataset  $S_k$ . By applying PCA to  $\Omega_k$ , an orthogonal transformation matrix  $P_k$  can be obtained. If we set  $P_k$  as the dictionary and let  $Z_k = P_k^T S_k$ , we will then have  $\|S_k - P_k Z_k\|_F^2 = \|S_k - P_k P_k^T S_k\|_F^2 = 0$ . In other words, the approximation term in (7) will be exactly zero, yet the corresponding sparsity regularization term  $\|Z_k\|_1$  will have a certain amount because all the representation coefficients in  $Z_k$  are preserved.

For a better balance between the  $l_1$ -norm regularization term and  $l_2$ -norm approximation term in (7), we consider only the first  $r$  most important eigenvectors in  $P_k$  to form a dictionary  $\Phi_r$ , i.e.,  $\Phi_r = [p_1, p_2, \dots, p_r]$ . Let  $\Lambda_r = \Phi_r^T S_k$ . Clearly, since not all of the eigenvectors are used to form  $\Phi_r$ , the reconstruction error  $\|S_k - \Phi_r \Lambda_r\|_F^2$  in (7) will increase with the decrease of  $r$ . However, the term  $\|\Lambda_r\|_1$  will decrease. Therefore, the optimal value of  $r$ , denoted by  $r_o$ , can be determined by

$$r_o = \arg \min_r \{ \|S_k - \Phi_r \Lambda_r\|_F^2 + \lambda \|\Lambda_r\|_1 \} \quad (8)$$

Finally, the subdictionary learned from subdataset  $S_k$  is  $\Phi_k = [p_1, p_2, \dots, p_{r_o}]$ .

Applying the above procedures to all of the  $K$  subdatasets  $S_k$ , we could get  $K$  subdictionaries  $\Phi_k$ , which will be used in the ASDS process of each given image patch.

### B. Adaptive Selection of the Subdictionary

We have learned a dictionary  $\Phi_k$  for each subset  $S_k$  in the above subsection. Meanwhile, we have computed the centroid  $\mu_k$  of each cluster  $C_k$  associated with  $S_k$ . Therefore, we have  $K$  pairs  $\{\Phi_k, \mu_k\}$ , with which the ASDS of each given image patch can be accomplished. In the proposed sparsity-based IR scheme, we assign adaptively a subdictionary to each local patch of  $X$ , spanning the adaptive sparse domain. Since  $X$  is unknown beforehand, we need to have an initial estimation of it. The initial estimation of  $X$  can be accomplished by taking

wavelet bases as the dictionary and then solving (6) with the iterated shrinkage algorithm in [10]. Let  $\hat{X}$  be the estimate of  $X$  and  $\hat{X}_i$  be a local patch of  $\hat{X}$ . Recall that we have the centroid  $\mu_k$  of each cluster available, and hence we could select the best fitted subdictionary to  $\hat{X}_i$  by comparing the high-pass filtered patch of  $\hat{X}_i$ , denoted by  $\hat{X}_i^h$ , to the centroid  $\mu_k$ . For example, we can select the dictionary for  $\hat{X}_i$  based on the minimum distance between  $\hat{X}_i^h$  and  $\mu_k$ , i.e.,

$$k_i = \arg \min_k \|\hat{X}_i^h - \mu_k\|_2 \dots \quad (9)$$

However, directly calculating the distance between  $\hat{X}_i^h$  and  $\mu_k$  may not be robust enough because the initial estimate  $\hat{X}$  can be noisy. Here, we propose to determine the subdictionary in the subspace of  $\mu_k$ . Let  $U = [\mu_1, \mu_2, \dots, \mu_k]$  be the matrix containing all the centroids. By applying SVD to the co-variance matrix of  $U$ , we can obtain the PCA transformation matrix of  $U$ . Let  $\Phi_c$  be the projection matrix composed by the first several most significant eigenvectors. We compute the distance between  $\hat{X}_i^h$  and  $\mu_k$  in the subspace spanned by  $\Phi_c$  as

$$k_i = \arg \min_k \|\Phi_c \hat{X}_i^h - \Phi_c \mu_k\|_2 \quad (10)$$

Compared with (9), (10) can increase the robustness of adaptive dictionary selection. By using (10), the  $k_i$  th subdictionary  $\Phi_{k_i}$  will be selected and assigned to patch  $\hat{X}_i$ . Then, we can update the estimation  $X$  of by minimizing (6) and letting  $\hat{X} = \Phi \circ \hat{\alpha}$ . With the updated estimate  $\hat{X}$ , the ASDS of  $X$  can be consequently updated. Such a process is iteratively implemented until the estimation  $\hat{X}$  converges.

### C. Adaptively Reweighted Sparsity Regularization

In (6), the parameter  $\lambda$  is a constant to weight the  $l_1$ -norm sparsity regularization term. Here, we propose a new method to estimate adaptively the image local sparsity and then reweight the  $l_1$ -norm sparsity in the ASDS scheme.

The reweighted  $l_1$ -norm sparsity regularized minimization with ASDS can be formulated as follows:

$$\hat{\alpha} = \arg \min_{\alpha} \{ \|y - DH\Phi \circ \alpha\|_2^2 + \sum_{i=1}^N \sum_{j=1}^n \lambda_{i,j} |\alpha_{i,j}| \} \quad (11)$$

where  $\alpha_{i,j}$  is the coefficient associated with the  $j$ th atom of  $\Phi_{k_i}$  and  $\lambda_{i,j}$  is the weight assigned to  $\alpha_{i,j}$ . In [13],  $\lambda_{i,j}$  is empirically computed as  $\lambda_{i,j} = 1 / (|\hat{\alpha}_{i,j}| + \epsilon)$ , where  $\hat{\alpha}_{i,j}$  is the estimate of  $\alpha_{i,j}$  and  $\epsilon$  is a small

constant. Here, we propose a more robust method for computing  $\lambda_{i,j}$  by formulating the sparsity estimation as a maximum a posterior (MAP) estimation problem. Under the Bayesian framework, with the observation  $Y$  the MAP estimation of  $\alpha$  is given by

$$\hat{\alpha} = \arg \max_{\alpha} \{\log P(\alpha|Y)\} \\ = \arg \min_{\alpha} \{-\log P(Y|\alpha) - \log P(\alpha)\}. \quad (12)$$

By assuming  $Y$  is contaminated with additive Gaussian white noises of standard deviation  $\sigma_n$ , we have

$$P(Y|\alpha) = \frac{1}{\sigma_n \sqrt{2\pi}} \exp\left(-\frac{1}{2\sigma_n^2} \|Y - D\mathcal{H}\Phi \circ \alpha\|_2^2\right) \quad (13)$$

The prior distribution  $P(\alpha)$  is often characterized by an i.i.d. zero-mean Laplacian probability model

$$P(\alpha) = \prod_{i=1}^N \prod_{j=1}^n \frac{1}{\sqrt{2}\sigma_{i,j}} \exp\left(-\frac{\sqrt{2}}{\sigma_{i,j}} |\alpha_{i,j}|\right) \quad (14)$$

where  $\sigma_{i,j}$  is the standard deviation of  $\alpha_{i,j}$ . By plugging  $P(Y|\alpha)$  and  $P(\alpha)$  into (12), we could readily derive the desired weight in (11) as  $\lambda_{i,j} = 2\sqrt{2}\sigma_n^2 / \sigma_{i,j}$ . For numerical stability, we compute the weights by

$$\lambda_{i,j} = \frac{2\sqrt{2}\sigma_n^2}{\hat{\sigma}_{i,j} + \epsilon} \quad (15)$$

where  $\hat{\sigma}_{i,j}$  is an estimate of  $\sigma_{i,j}$  and  $\epsilon$  is a small constant. Now, let us discuss how to estimate  $\sigma_{i,j}$ . Let  $\hat{X}_i$  be the estimate of  $X_i$  and  $\hat{X}_i^l, l=1,2,\dots,L$ , be the nonlocal similar patches to  $\hat{X}_i$ . (The determination of nonlocal similar patches to  $\hat{X}_i$  will be described in Section IV-C.) The representation coefficients of these similar patches over the selected subdictionary  $\Phi_{k_i}$  is  $\hat{\alpha}_i^l = \Phi_{k_i}^T \hat{X}_i^l$ . Then, we can estimate  $\sigma_{i,j}$  by calculating the standard deviation of each element  $\hat{\alpha}_{i,j}^l$  in  $\hat{\alpha}_i^l$ .

**SPATIALLY ADAPTIVE REGULARIZATION**

In the above Section, we proposed to select adaptively a subdictionary to code the given image patch. To further improve the IR method we introduce two types of adaptive regularization (AReg) terms. A local area in a natural image can be viewed as a stationary process, which can be well modeled by the autoregressive (AR) models. Here, we propose to learn a set of AR models from the clustered high quality training image patches, and adaptively select one AR model to regularize the input image patch. Besides the AR models, which exploit the image local correlation, we

propose to use the nonlocal similarity constraint as a complementary AReg term to the local AR models.

**Training the AR Models**

Recall that, in the above Section, we have partitioned the whole training dataset into  $K$  subdatasets  $S_k$ . For each  $S_k$ , an AR model can be trained using all of the sample patches inside it. Here we let the support of the AR model be a square window, and the AR model aims to predict the central pixel of the window by using the neighboring pixels. Considering that determining the best order of the AR model is not trivial, and a high order AR model may cause data over-fitting, in our experiments a  $3 \times 3$  window (i.e., AR model of order 8) is used. The vector of AR model parameters, denoted by  $a_k$ , of the  $k^{\text{th}}$  subdataset  $S_k$ , can be easily computed by solving the following least square problem:

$$a_k = \arg \min_a \sum_{s_i \in S_k} (s_i - a^T q_i)^2 \quad (16)$$

where  $s_i$  is the central pixel of image patch  $s_i$  and  $q_i$  is the vector that consists of the neighboring pixels of  $s_i$  within the support of the AR model. By applying the AR model training process to each subdataset, we obtain a set of AR models  $\{a_1, a_2, \dots, a_K\}$  that are used for adaptive regularization.

**A. Adaptive Selection of the AR Model for Regularization**

The adaptive selection of the AR model for each patch  $X_i$  is similar to the selection of a subdictionary for  $X_i$  described in Section Adaptive Selection of the sub-dictionary. With an estimation  $\hat{X}_i$  of  $X_i$ , we compute its high-pass Gaussian filtering output  $\hat{X}_i^h$ . Let  $k_i = \arg \min_k \|\Phi_c \hat{X}_i^h - \Phi_c \mu_k\|_2$ , and then the  $k_i^{\text{th}}$  AR model  $a_{k_i}$  will be assigned to patch  $X_i$ . Denote by  $X_i$  the central pixel of patch  $X_i$  and by  $\chi_i$  the vector containing the neighboring pixels of  $X_i$  within patch  $X_i$ . We can expect that the prediction error of  $X_i$  using  $a_{k_i}$  and  $\chi_i$  should be small, i.e.,  $\|X_i - a_{k_i}^T \chi_i\|_2^2$  should be minimized. By incorporating this constraint into the ASDS-based sparse representation model in (11), we have a lifted objective function as follows:

$$\hat{\alpha} = \arg \min_{\alpha} \left\{ \|Y - D\mathcal{H}\Phi \circ \alpha\|_2^2 + \sum_{i=1}^N \sum_{j=1}^n \lambda_{i,j} |\alpha_{i,j}| + \gamma \sum_{X_i \in X} \|X_i - a_{k_i}^T \chi_i\|_2^2 \right\} \quad (17)$$

where  $\gamma$  is a constant balancing the contribution of the AR regularization term. For the convenience of expression, we

write the third term  $\sum_{X_i \in X} \|X_i - a_{k_i}^T \chi_i\|_2^2$  as  $\|(I - A)X\|_2^2$ , where I is the identity matrix and

$$A_{(i,j)} = \begin{cases} a_i, & \text{if } X_i \text{ is an element of } \chi_i, a_i \in a_{k_i} \\ 0, & \text{otherwise.} \end{cases}$$

Then, (17) can be rewritten as

$$\hat{\alpha} = \underset{\alpha}{\operatorname{argmin}} \left\{ \|Y - DH\Phi \circ \alpha\|_2^2 + \sum_{i=1}^N \sum_{j=1}^n \lambda_{i,j} |\alpha_{i,j}| + \gamma \cdot \|(I - A)X\|_2^2 \right\} \quad (18)$$

**B. Adaptive Regularization by Nonlocal Similarity**

The above discussed AR model-based AReg exploits the local statistics in each image patch. On the other hand, there are often many repetitive patterns throughout a natural image. Such nonlocal redundancy is very helpful to improve the quality of reconstructed images. As a complementary AReg term to AR models, we further introduce a nonlocal similarity regularization term into the sparsity-based IR framework.

For each local patch  $X_i$ , we search for the similar patches to it in the whole image X (in practice, in a sufficiently large area around  $X_i$ ). A patch  $X_i^l$  is selected as a similar patch to  $X_i$  if  $e_i^l = \|\widehat{X}_i - \widehat{X}_i^l\|_2^2 \leq t$ , where t is a preset threshold, and  $\widehat{X}_i$  and  $\widehat{X}_i^l$  are the current estimates of  $X_i$  and  $X_i^l$ , respectively, or we can select the patch  $\widehat{X}_i^l$  if it is within the first L (L=10 in our experiments) closest patches to  $\widehat{X}_i$ . Let  $X_i$  be the central pixel of patch  $X_i$ , and  $X_i^l$  be the central pixel of patch  $X_i^l$ . Then, we can use the weighted average of  $X_i^l$  i.e.,  $\sum_{l=1}^L b_i^l X_i^l$ , to predict  $X_i$ ,

and the weight  $b_i^l$  assigned to  $X_i^l$  is set as  $b_i^l = \exp(-e_i^l / h) / c_i$ , where h is a controlling factor of the weight and  $c_i = \sum_{l=1}^L \exp(-e_i^l / h)$  is the normalization factor. Considering that there is much nonlocal redundancy in natural images, we expect that the prediction error  $\|X_i - \sum_{l=1}^L b_i^l X_i^l\|_2^2$  should be small. Let  $b_i$  be the column

vector containing all the weights  $b_i^l$  and  $\beta_i$  be the column vector containing all  $X_i^l$ . By incorporating the nonlocal similarity regularization term into the ASDS based sparse representation in (11), we have

$$\hat{\alpha} = \underset{\alpha}{\operatorname{argmin}} \left\{ \|Y - DH\Phi \circ \alpha\|_2^2 + \sum_{i=1}^N \sum_{j=1}^n \lambda_{i,j} |\alpha_{i,j}| + \eta \cdot \sum_{X_i \in X} \|X_i - b_i^T \beta_i\|_2^2 \right\} \quad (19)$$

where  $\eta$  is a constant balancing the contribution of nonlocal regularization. Equation (19) can be rewritten as  $\hat{\alpha} = \underset{\alpha}{\operatorname{argmin}} \left\{ \|Y - DH\Phi \circ \alpha\|_2^2 + \sum_{i=1}^N \sum_{j=1}^n \lambda_{i,j} |\alpha_{i,j}| + \eta \cdot \|(I - B)\Phi \alpha\|_2^2 \right\}$  (20)

where I is the identity matrix and

$$B(i,l) = \begin{cases} b_i^l, & \text{if } X_i^l \text{ is an element of } \beta_i, b_i^l \in b_i \\ 0, & \text{otherwise} \end{cases}$$

**SUMMARY OF THE ALGORITHM**

After including both the local AR regularization and the nonlocal similarity regularization into the ASDS-based sparse representation in (11), we have the following ASDS-AReg-based sparse representation to solve the IR problem:

$$\hat{\alpha} = \underset{\alpha}{\operatorname{argmin}} \left\{ \|Y - DH\Phi \circ \alpha\|_2^2 + \gamma \cdot \|(I - A)\Phi \circ \alpha\|_2^2 + \sum_{i=1}^N \sum_{j=1}^n \lambda_{i,j} |\alpha_{i,j}| + \eta \cdot \|(I - B)\Phi \circ \alpha\|_2^2 \right\} \quad (21)$$

In (21), the first  $l_2$ -norm term is the fidelity term, guaranteeing that the solution  $\widehat{X} = \Phi \circ \hat{\alpha}$  can well fit the observation Y after degradation by operators H and D; the second  $l_2$ -norm term is the local AR model-based adaptive regularization term, requiring that the estimated image is locally stationary; the third  $l_2$ -norm term is the nonlocal similarity regularization term, which uses the nonlocal redundancy to enhance each local patch; and the last weighted  $l_1$ -norm term is the sparsity penalty term, requiring that the estimated image should be sparse in the adaptively selected domain. Equation (21) can be rewritten as

$$\hat{\alpha} = \underset{\alpha}{\operatorname{argmin}} \left\{ \begin{bmatrix} Y \\ 0 \\ 0 \end{bmatrix} - \begin{bmatrix} DH \\ \gamma \cdot (I - A) \\ \eta \cdot (I - B) \end{bmatrix} \Phi \circ \alpha \right\|_2^2 + \sum_{i=1}^N \sum_{j=1}^n \lambda_{i,j} |\alpha_{i,j}| \quad (22)$$

By letting

$$\widetilde{Y} = \begin{bmatrix} Y \\ 0 \\ 0 \end{bmatrix} \quad K = \begin{bmatrix} DH \\ \gamma \cdot (I - A) \\ \eta \cdot (I - B) \end{bmatrix} \quad (23)$$

(22) can be rewritten as

$$\hat{\alpha} = \underset{\alpha}{\operatorname{argmin}} \left\{ \|\widetilde{Y} - K\Phi \circ \alpha\|_2^2 + \sum_{i=1}^N \sum_{j=1}^n \lambda_{i,j} |\alpha_{i,j}| \right\} \quad (24)$$

This is a reweighted  $l_1$ -minimization problem, which can be effectively solved by the iterative shrinkage algorithm [8]. We outline the iterative shrinkage algorithm for optimizing (24) in Algorithm 1.

**Algorithm 1**

**1) Initialization:**

- a) By taking the wavelet domain as the sparse domain, we can compute an initial estimate, denoted by  $\widehat{X}$ , of X by using the iterated wavelet shrinkage algorithm [8];
- b) With the initial estimate  $\widehat{X}$ , we select the subdictionary  $\Phi_{k_i}$  and the AR model  $a_i$  using (10), and calculate the nonlocal weight  $b_i$  for each local patch  $\widehat{X}_i$ ;
- c) Initialize A and B with the selected AR models and the nonlocal weights;
- d) Preset  $\gamma, \eta, P, e$  and the maximal iteration number, denoted by Max\_Iter;
- e) Set  $k=0$ .

2) Iterate on k until  $\|\widehat{X}^{(k)} - \widehat{X}^{(k+1)}\|_2^2 / N \leq e$  or  $k \geq \text{Max\_Iter}$  is satisfied.

a) 
$$\widehat{X}^{(k+1/2)} = \widehat{X}^{(k)} + K^T (\widetilde{Y} - K\widehat{X}^{(k)}) = \widehat{X}^{(k)} + (UY - U\widehat{X}^{(k)}) / (V + U^T U)$$
, where  $U = (DH)^T DH$  and  $V = \gamma^2 (I - A)^T (I - A) + \eta^2 (I - B)^T (I - B)$ ;

b) Compute  $\alpha^{(k+1/2)} = [\Phi_{k_1}^T R_1 \widehat{X}^{(k+1/2)}, \dots, \Phi_{k_N}^T R_N \widehat{X}^{(k+1/2)}]$ , where N is the total number of image patches;

c)  $\widehat{\alpha}_{i,j}^{(k+1)} = \text{soft}(\alpha_{i,j}^{(k+1/2)}, \tau_{i,j})$ , where  $\text{soft}(\cdot, \tau_{i,j})$  is a soft thresholding function with threshold  $\tau_{i,j}$ ;

d) Compute  $\widehat{X}^{(k+1)} = \Phi \circ \alpha^{(k+1)}$  using (5), which can be calculated by first reconstructing each image patch with  $\widehat{X}_i = \Phi_{k_i} \alpha_i^{(k+1)}$  and then averaging all the reconstructed image patches;

e) If  $\text{mod}(k,P) = 0$ , update the adaptive sparse domain of X and the matrices A and B using the improved estimate  $\widehat{X}^{(k+1)}$ .

In Algorithm 1, e is a prespecified scalar controlling the convergence of the iterative process, and Max\_Iter is the allowed maximum number of iterations. The thresholds  $\tau_{i,j}$  are locally computed as  $\tau_{i,j} = \lambda_{i,j} / r$  [8], where  $\lambda_{i,j}$  are calculated by (15) and r is chosen such that  $r > \|(K\Phi)^T K\Phi\|_2$ . Since the dictionary  $\Phi_{k_i}$  varies across the image, the optimal determination of r for each local patch is difficult. Here, we empirically set  $r=4.7$  for all of the patches. P is a preset integer, and we only update the subdictionaries  $\Phi_{k_i}$ , the AR models  $a_i$  and the weights  $b_i$  in every P iterations to save computational cost. With the updated  $a_i$  and  $b_i$ , A and B can be updated, and then the matrix V can be updated.

**Centralised Sparse Representation:**

The equation for CSR model can be written as:

$$\alpha_Y = \arg \min_Y \{ \|Y - H\Phi \circ \alpha\|_2^2 + \lambda \|\alpha\|_1 + \gamma \sum_{i=1}^N \|\alpha_i - \mu_i\|_p,$$

where  $\mu_i = \sum_{j \in C_i} w_{i,j} \alpha_{i,j}$  (where  $w_{i,j}$  is the weight,  $w_{i,j}$  can be set to be inverse proportional to the distance between patches i and j:

$$w_{i,j} = \exp(-\|\widehat{X}_i - \widehat{X}_{i,j}\|_2^2 / h) / W$$

where  $\widehat{X}_i = \Phi \widehat{\alpha}_i$  and  $\widehat{X}_{i,j} = \Phi \widehat{\alpha}_{i,j}$  are the estimates of patches i and j, W is a normalization factor and h is a predetermined scalar.  $\|\cdot\|_p$  is l-p norm and p=0 or 1, From above Eq we can more clearly see that the CSR model

unifies the local sparsity (i.e.  $\|\alpha\|_1$ ) and nonlocal similarity induced sparsity (i.e.  $\|\alpha_i - \mu_i\|_p$ ) into a unified variational formulation. By exploiting both the local and nonlocal redundancy, better IR results can be expected.

**EXPERIMENTAL RESULTS**

To illustrate the robustness of the proposed method to the training dataset, we use two different sets of training images in the experiments, each set having five high-quality images as shown in Fig. 1. We can see that these two sets of training images are very different in contents. We use  $\text{Var}(s_i) > \Delta$  with  $\Delta = 16$  to exclude the smooth image patches, and a total amount of 727 615 patches of size  $7 \times 7$  are randomly cropped from each set of training images. In the experiments of deblurring, two types of blur kernels, a Gaussian kernel of standard deviation 3 and a  $9 \times 9$  uniform kernel, were used to simulate blurred images. Additive Gaussian white noises with standard deviations  $\sqrt{2}$  was then added to the blurred images, respectively. In the experiments of super-resolution, the degraded LR images were generated by first applying a truncated  $7 \times 7$  Gaussian kernel of standard deviation 1.6 to the original image and then down-sampling by a factor of 3. In both of the deblurring and super-resolution experiments,  $7 \times 7$  patches (for HR image) with 5-pixel- width overlap between adjacent patches were used in the proposed methods. For color images, all of the test methods were applied to the luminance component only because human visual system is more sensitive to luminance changes, and the bi-cubic interpolator was applied to the chromatic components. Here we only report the PSNR and SSIM [12] results for the luminance component. To examine more comprehensively the proposed approach, we give three results of the proposed method: the results by using only ASDS (denoted by ASDS), by using ASDS plus AR regularization (denoted by ASDS-AR), and by using ASDS with both AR and nonlocal similarity regularization (denoted by ASDS-AR-NL), CSR.

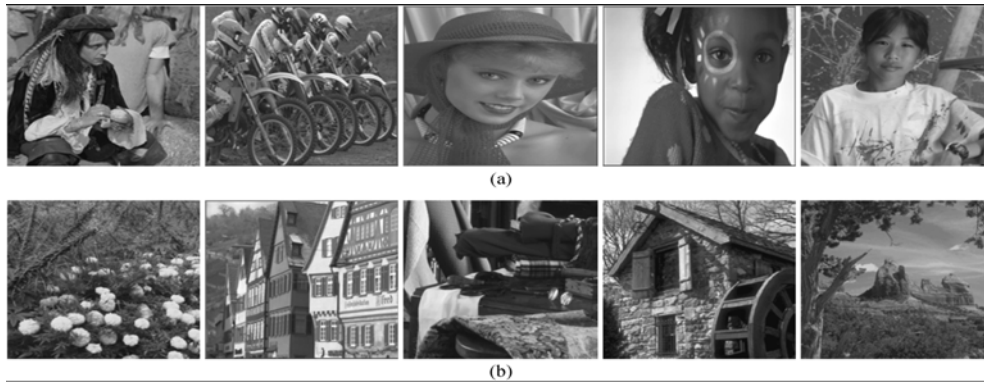


Fig 1 Two sets of high-quality images used for training subdictionaries and AR models. (a) Training dataset 1. (b) Training dataset 2. We see that the two training datasets are very different in the contents.



Fig:2 Comparison of the deblurred images on *barbara* by different methods on training dataset 1 (Gaussian blur kernel and  $\sigma_n = \sqrt{2}$ ). Original, degraded, ASDS method (PSNR=26.85dB, SSIM=0.7791), the ASDS\_AR method (PSNR= 27.14dB, SSIM=0.7934), the ASDS\_AR\_NL method (PSNR=27.92dB, SSIM=0.8263), the CSR method (PSNR=27.98 dB, SSIM=0.8216).



Fig:3 Comparison of the deblurred images on *hat* by different methods on training dataset 2 (uniform blur kernel and  $\sigma_n = \sqrt{2}$ ). Original, degraded, ASDS method (PSNR=31.54dB, SSIM=0.8675), the ASDS\_AR method (PSNR= 31.47dB, SSIM=0.8660), the ASDS\_AR\_NL method (PSNR=31.55dB, SSIM=0.8659), the CSR method (PSNR=31.95 dB, SSIM=0.8742).



Fig:4 Comparison of the super-resolution images on *plants* by different methods on training dataset 1 (scaling factor=3). Original, degraded, ASDS method (PSNR=33.07dB, SSIM=0.9025), the ASDS\_AR method (PSNR=33.02dB, SSIM=0.9019), the ASDS\_AR\_NL method (PSNR=33.40dB, SSIM=0.9072), the CSR method (PSNR= 34.11dB, SSIM=0.9217).



Fig:5 Comparison of the super-resolution images on noisy girl by different methods on training dataset 2 (scaling factor=3). Original, degraded, ASDS method (PSNR=33.39dB, SSIM=0.8190), the ASDS\_AR method (PSNR=33.40dB, SSIM=0.8192), the ASDS\_AR\_NL method (PSNR=33.47dB, SSIM=0.8200), the CSR method (PSNR= 33.68dB, SSIM=0.8258).

The above figures gives the comparison results of deblurring and super-resolution reconstructed by using ASDS, ASDS\_AR, ASDS\_AR\_NL and CSR methods and their PSNR, SSIM values. The tables below gives the results

of deblurring and super-resolution for different images in terms of PSNR and SSIM values on Training dataset 1 and Training dataset 2 respectively.



Images	ASDS-TD1	ASDS-TD2	ASDS-AR-TD1	ASDS-AR-TD2	ASDS-AR-NL-TD1	ASDS-AR-NL-TD2	CSR
Barbara	26.85	26.80	27.14	27.09	27.92	27.90	27.98
	0.7791	0.7765	0.7934	0.7925	0.8263	0.8258	0.8216
Bike	25.57	25.53	25.47	25.43	25.54	25.50	25.85
	0.8119	0.8103	0.8089	0.8072	0.8095	0.8075	0.8218
Parrots	31.27	31.23	31.15	31.13	31.20	31.20	32.05
	0.8997	0.8998	0.8988	0.8988	0.8984	0.8984	0.9111
Baboon	21.41	21.41	21.51	21.50	21.58	21.58	21.56
	0.5845	0.5840	0.5835	0.5824	0.5740	0.5741	0.5824
Pentagon	25.66	25.65	25.91	25.91	26.61	26.60	26.69
	0.7257	0.7242	0.7343	0.7332	0.7561	0.7548	0.7587
Boats	28.84	28.80	29.36	29.33	30.78	30.76	31.10
	0.8033	0.8010	0.8233	0.8221	0.8677	0.8671	0.8816
Cameraman	27.19	27.15	27.37	27.37	28.12	28.10	28.54
	0.7860	0.7838	0.8103	0.8137	0.8546	0.8548	0.8561
Hat	31.61	31.54	31.54	31.47	31.58	31.55	31.95
	0.8678	0.8675	0.8666	0.8660	0.8655	0.8659	0.8742
Peppers	28.09	28.10	28.47	28.47	29.44	29.44	29.66
	0.7670	0.7672	0.7883	0.7892	0.8344	0.8350	0.8406
Straw	22.32	22.31	22.41	22.41	22.54	22.52	22.76
	0.6681	0.6658	0.6667	0.6642	0.6570	0.6550	0.6705

Table:1PSNR and SSIM results of Deblurred Images (Uniform Blur Kernel ,Noise Level  $\sigma_n = \sqrt{2}$  )

Images	ASDS-TD1	ASDS-TD2	ASDS-AR-TD1	ASDS-AR-TD2	ASDS-AR-NL-TD1	ASDS-AR-NL-TD2	CSR
Barbara	23.82	23.81	23.82	23.81	23.85	23.84	27.77
	0.6598	0.6593	0.6602	0.6597	0.6637	0.6632	0.8252
Bike	22.66	22.63	22.65	22.63	22.82	22.81	27.59
	0.6727	0.6707	0.6728	0.6708	0.6843	0.6831	0.8842
Parrots	27.78	27.75	27.84	27.81	27.95	27.91	33.45
	0.8629	0.8620	0.8631	0.8622	0.8676	0.8668	0.9361
Baboon	20.11	20.09	20.10	20.08	20.12	20.11	21.55
	0.3880	0.3874	0.3886	0.3880	0.3950	0.3933	0.5956
Pentagon	23.71	23.71	23.70	23.71	23.75	23.74	27.79
	0.5990	0.5978	0.5995	0.5987	0.6103	0.6088	0.8284
Boats	26.91	26.93	27.01	27.01	27.12	27.13	31.43
	0.7677	0.7675	0.7675	0.7672	0.7697	0.7696	0.8941
Cameraman	24.07	24.06	24.04	24.04	24.21	24.21	28.29
	0.7596	0.7603	0.7584	0.7595	0.7600	0.7605	0.8561
Hat	28.79	28.83	28.82	28.83	28.94	28.94	33.09
	0.8022	0.8034	0.8016	0.8030	0.8051	0.8064	0.9026
Peppers	26.29	26.28	26.25	26.26	26.38	26.40	30.20
	0.7822	0.7865	0.7874	0.7864	0.7890	0.7880	0.8673
Straw	20.74	20.74	20.76	20.76	20.86	20.85	25.47
	0.4757	0.4749	0.4781	0.4775	0.4881	0.4873	0.8383

Table:2 PSNR and SSIM results of Deblurred Images (Gaussian Blur Kernel ,Noise Level  $\sigma_n = \sqrt{2}$  )

Images	ASDS(TD1)	ASDS(TD2)	ASDS-AR(TD1)	ASDS-AR(TD2)	ASDS-AR-NL(TD1)	ASDS-AR-NL(TD2)	CSR
Parrot	29.75	29.75	29.80	29.80	30.10	30.09	30.63
	0.9071	0.9066	0.9070	0.9065	0.9099	0.9100	0.9181
Hat	30.91	30.82	30.84	30.76	31.01	30.99	31.35
	0.8694	0.8681	0.8684	0.8671	0.8716	0.8713	0.8738
Bike	24.33	24.60	24.28	24.31	24.61	24.26	24.72
	0.7855	0.7959	0.7835	0.7844	0.7962	0.7826	0.8029
Butterfly	26.74	26.69	26.65	26.59	27.35	27.30	28.24
	0.8939	0.8923	0.8909	0.8893	0.9057	0.9048	0.9219
Flower	28.90	28.89	28.90	28.88	29.17	29.17	29.55
	0.8386	0.8377	0.8385	0.8375	0.8464	0.8462	0.8586
Girl	33.41	33.39	33.40	33.40	33.47	33.47	33.68
	0.8193	0.8190	0.8193	0.8192	0.8201	0.8200	0.8258
Leaves	26.25	26.22	26.17	26.17	26.92	26.92	27.59
	0.8947	0.8940	0.8927	0.8924	0.9094	0.9095	0.9273
Parthenon	26.74	26.75	26.73	26.75	26.89	26.89	27.23
	0.7322	0.7326	0.7317	0.7326	0.7367	0.7366	0.7524
Plants	33.07	33.05	33.02	33.00	33.40	33.40	34.11
	0.9025	0.9020	0.9019	0.9014	0.9072	0.9070	0.9217
Raccoon	29.13	29.11	29.14	29.10	29.25	29.22	29.30
	0.7650	0.7633	0.7653	0.7636	0.7669	0.7654	0.7677

Table:3 PSNR and SSIM results of reconstructed HR images (Noise Level  $\sigma_n = 0$  )

Images	ASDS(TD1)	ASDS(TD2)	ASDS-AR(TD1)	ASDS-AR(TD2)	ASDS-AR-NL(TD1)	ASDS-AR-NL(TD2)	CSR
Noisy Parrot	28.92 0.8684	28.90 0.8679	28.81 0.8633	28.78 0.8633	28.74 0.8653	28.72 0.8655	29.50 0.8775
Noisy Hat	29.61 0.8087	29.61 0.8097	29.50 0.8070	29.50 0.8084	29.57 0.8131	29.57 0.8147	29.96 0.8249
Noisy Bike	23.60 0.7234	23.58 0.7222	23.48 0.7197	23.48 0.7186	23.53 0.7208	23.52 0.7197	23.77 0.7363
Noisy Butterfly	25.76 0.8417	25.78 0.8406	25.57 0.8367	26.02 0.8604	26.01 0.8600	26.01 0.8603	26.89 0.8887
Noisy Flower	27.58 0.7685	27.54 0.7665	27.64 0.7705	27.62 0.7700	27.67 0.7744	27.66 0.7742	28.07 0.7936
Noisy Girl	31.69 0.7574	31.72 0.7591	31.70 0.7578	31.72 0.7591	31.76 0.7585	31.77 0.7589	32.04 0.7642
Noisy Leaves	25.22 0.8471	25.14 0.8455	25.09 0.8430	25.05 0.8425	25.47 0.8628	25.50 0.8637	26.24 0.8949
Noisy Parthenon	26.09 0.6842	26.12 0.6855	26.06 0.6819	26.08 0.6833	26.07 0.6803	26.08 0.6814	26.42 0.7008
Noisy Plants	30.94 0.8288	30.95 0.8292	30.89 0.8285	30.91 0.8291	31.06 0.8348	31.06 0.8344	31.81 0.8606
Noisy Raccoon	27.99 0.6883	27.98 0.6882	28.00 0.6880	27.98 0.6871	28.00 0.6815	27.99 0.6814	28.02 0.6812

Table:4 PSNR and SSIM results of reconstructed HR images (Noise Level  $\sigma_n = 5$ )

### CONCLUSION

Image restoration (IR) is a fundamental topic in image processing and computer vision applications, and it has been widely studied. In this paper, we investigated IR with the sparse coding techniques. A novel sparse representation-based image deblurring and (single-image) super-resolution method using adaptive sparse domain selection (ASDS) and adaptive regularization (AReg), Centralised Sparse Representation (CSR). Since the optimal sparse domains of natural images can vary significantly across different images and different image patches in a single image, we selected adaptively the dictionaries that were prelearned from a dataset of high-quality example patches for each local patch. To further improve the quality of reconstructed images (reconstructed by using ASDS), we introduced two AReg terms into the ASDS based image restoration framework. One is a set of autoregressive (AR) models were learned from the training dataset and were used to regularize the image local smoothness. The image nonlocal similarity was incorporated as another regularization term to exploit the image nonlocal redundancies. An iterated shrinkage algorithm was proposed to implement the proposed ASDS algorithm with AReg. To further enhance the quality of the reconstructed images we introduced the concept of sparse coding noise (SCN), and it was empirically found that SCN follows Laplacian distributions. To suppress SCN and thus improve the quality of IR, the centralized sparse representation (CSR) model was proposed by exploiting the image nonlocal self-similarity. The experimental results on natural images showed that the proposed approach can significantly outperform other leading IR methods in both PSNR and visual quality (SSIM).

### REFERENCES

- [1] Weisheng Dong, Lei Zhang, Guangming Shi, Xiaolin Wu, "Image Deblurring and Super-Resolution by Adaptive Sparse Domain Selection and Adaptive Regularization", *IEEE TRANSACTIONS ON IMAGE PROCESSING*, VOL. 20, NO. 7, JULY 2011
- [2] M. Bertero and P. Boccacci, *Introduction to Inverse Problems in Imaging*. Bristol, U.K.: IOP, 1998.
- [3] D. Donoho, "Compressed sensing," *IEEE Trans. Inf. Theory*, vol. 52, no. 4, pp. 1289–1306, Apr. 2006.
- [4] E. Candès, J. Romberg, and T. Tao, "Robust uncertainty principles: Exact signal reconstruction from highly incomplete frequency information," *IEEE Trans. Inf. Theory*, vol. 52, no. 2, pp. 489–509, Feb. 2006.
- [5] M. R. Baham and A. K. Katsaggelos, "Digital image restoration," *IEEE Trans. Signal Process. Mag.*, vol. 14, no. 2, pp. 24–41, Mar. 1997.
- [6] L. Rudin, S. Osher, and E. Fatemi, "Nonlinear total variation based noise removal algorithms," *Phys. D*, vol. 60, pp. 259–268, 1992.
- [7] T. Chan, S. Esedoglu, F. Park, and A. Yip, "Recent developments in total variation image restoration," in *Mathematical Models of Computer Vision*, N. Paragios, Y. Chen, and O. Faugeras, Eds. New York: Springer-Verlag, 2005.
- [8] I. Daubechies, M. Defriese, and C. DeMol, "An iterative thresholding algorithm for linear inverse problems with a sparsity constraint," *Commun. Pure Appl. Math.*, vol. 57, pp. 1413–1457, 2004.
- [9] S. D. Babacan, R. Molina, and A. K. Katsaggelos, "Total variation super resolution using a variational approach," in *Proc. Int. Conf. Image Process.*, Oct. 2008, pp. 641–644.
- [10] D. L. Donoho, "De-noising by soft thresholding," *IEEE Trans. Inf. Theory*, vol. 41, no. 3, pp. 613–627, May 1995.
- [11] X. Wu, K. U. Barthel, and W. Zhang, "Piecewise 2-D autoregression for predictive image coding," in *Proc. Int. Conf. Image Process.*, Oct. 1998, vol. 3, pp. 901–904.
- [12] Z. Wang, A. C. Bovik, H. R. Sheikh, and E. P. Simoncelli, "Image quality assessment: From error measurement to structural similarity," *IEEE Trans. Image Process.*, vol. 3, no. 4, pp. 600–612, Apr. 2004.
- [13] E. Candès, M. B. Wakin, and S. P. Boyd, "Enhancing sparsity by reweighted  $\ell_1$  minimization," *J. Fourier Anal. Applic.*, vol. 14, pp. 877–905, Dec. 2008.
- [14] Lei Zhang a, Weisheng Dong a,b, David Zhang a, Guangming Shi b, "Two-stage image denoising by principal component analysis with local pixel grouping", L. Zhang et al. / *Pattern Recognition* 43 (2010) 1531–1549